



## INVESTIGATION OF GEOTHERMAL ENERGY POTENTIAL OF PARTS OF CENTRAL AND NORTH-EASTERN NIGERIA USING SPECTRAL ANALYSIS TECHNIQUE

\*<sup>1</sup>Odidi, I. G., <sup>2</sup>Mallam, A. and <sup>2</sup>Nasir, N.

<sup>1</sup>Integrated Science Department, School of Secondary Science Education, Federal College of Education Zaria, Kaduna State, Nigeria.

<sup>2</sup>Physics Department, Faculty of Science, University of Abuja, Nigeria

\*Corresponding Author's Email: [idenageorge@gmail.com](mailto:idenageorge@gmail.com)

### ABSTRACT

The current study deals with an estimate of the Curie point depth, heat flow and geothermal gradient from spectral analysis of aeromagnetic data covering an area located approximately between latitude 7.5° N to 11.5° N and longitude 7.5° E to 10.5° E, which corresponds to parts of the Benue trough (lower part of the Upper Benue trough, the entire middle Benue trough, and upper part of the Lower Benue trough), lower part of the Gongola and Yola Basins, the Precambrian Basement, the Jurassic Younger Granites and two prominent hot Springs, Wiki hot spring in Bauchi state (in the north-eastern part) and Akiri hot spring in Nasarawa state (in the south-western part) of central and north-eastern Nigeria. Radially power spectrum was applied to the aeromagnetic data of the study area divided into 48 square blocks and each block analysed using the spectral centroid method to obtain depth to the top, centroid and bottom of magnetic sources. The depth values were subsequently used to evaluate the Curie-point depth (CPD), geothermal gradient and near-surface heat flow in the study area. The values of the curie point depths ( $Z_b$ ), range from 7.6341 km to 34.5158 km, with a mean value of 14.7928 km, geothermal gradient, range from 16.8039 0C km<sup>-1</sup> to 75.97490C km<sup>-1</sup>, with mean value of 45.7021 0C km<sup>-1</sup> and heat flow ( $q$ ), range from 42.0097 mWm<sup>-2</sup> to 189.9372 mWm<sup>-2</sup>, with a mean value of 114.2554 mWm<sup>-2</sup>. Which reveals that, there might probably be good sources for geothermal and thereby further recommended for detailed geothermal exploration.

**Keywords:** Aeromagnetic data, Curie point depth, Heat flow, geothermal gradient

### INTRODUCTION

Nigeria is currently facing incessant problem of epileptic power supply, which has affected her Productivity, hence her inability as a Nation to compete socially, politically, economical, and technologically with other nations of the world. Nigeria's over dependence on oil and natural gas has constituted a hindrance towards the harnessing of other sources of power that can contribute immensely to the economic growth of the nation. In other to consistently generate electricity, other sources of power that are widely referred to as renewable energy emerging in the wake of climate change and the depletion of the ozone layer should be explored (Byerly and Stolt, 1977; Connard et al., 1983; Black, 1980; Kebede, 1986; Salem et al., 2000; Glassley, 2010; Shere, 2013). One of which is the geothermal energy. In the light of the above, the Nigeria nation has a lot to benefit from exploring its geothermal potential for the production of electricity in the country. This is the main aim of this study. Radially power spectrum was applied to the aeromagnetic data of the study area divided into 48 square blocks and each block analysed using the spectral centroid method to obtain depth to the top, centroid and bottom of magnetic sources. The estimated values were used to compute the curie point depth, the heat flow

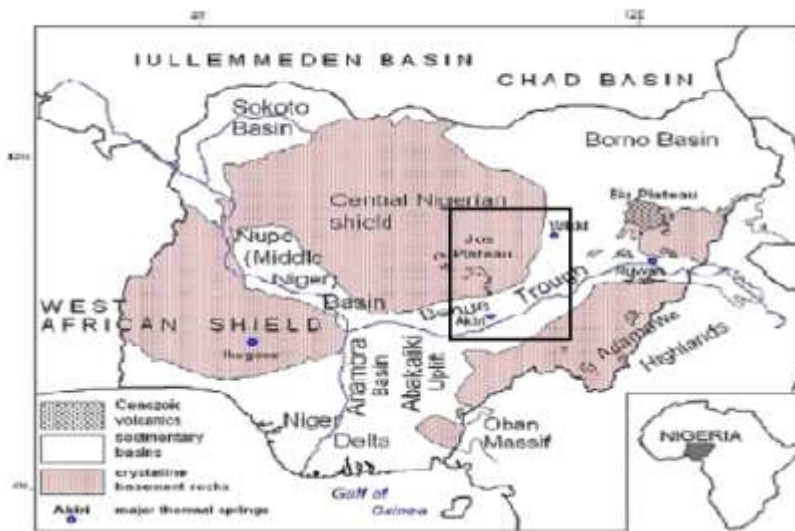
and thermal gradient of the area. The study area is bounded by latitudes 7.50°N to 11.50°N and longitudes 7.50°E to 10.50°E located within the central and northeast Nigeria (Fig.1, Fig.2 and Fig.3 & Fig.4). It is approximately 145,200 km<sup>2</sup> and was covered by 48 aeromagnetic maps (Chinwuko et al., 2013; Tildy, 2015; Alexander, 2017). The study area is made up of the cretaceous Benue trough, Precambrian basement Complex, Sedimentary Basins (Gongola and Yola Basins), Jurassic younger Granites, and tertiary – recent sediments of the central and north-eastern Nigeria (Fig.3 and Fig.4). Several works (Salako 2012; Nur et al., 1999; Eletta and Udensi 2012; Abdulsalam et al., 2013; Ikumbur et al., 2013; Igwesi and Umego 2013; Bello et al., 2017; Mohammed et al., 2019; Abdullahi et al., 2019) have been done in parts of the, north central, north eastern Nigeria but they are all restricted or localized to small areas around hot springs and a few on regional scale in the present study area (Fig.1 and Fig.2). The geology of the study area is made up of the cretaceous Benue trough, Precambrian basement Complex, Sedimentary Basins (Gongola and Yola Basins), Jurassic younger Granites, and tertiary – recent sediments of the central and north-eastern Nigeria

(Kogbe 1989; Ekwueme, 1987; Reymont, 1965; Carter et al., 1963; Farnbauer and Tietz, 2000; Adelana et al., 2008). (Fig.3



 Study area

Fig.1: Map of the study area (modified after NGSA, 2010)





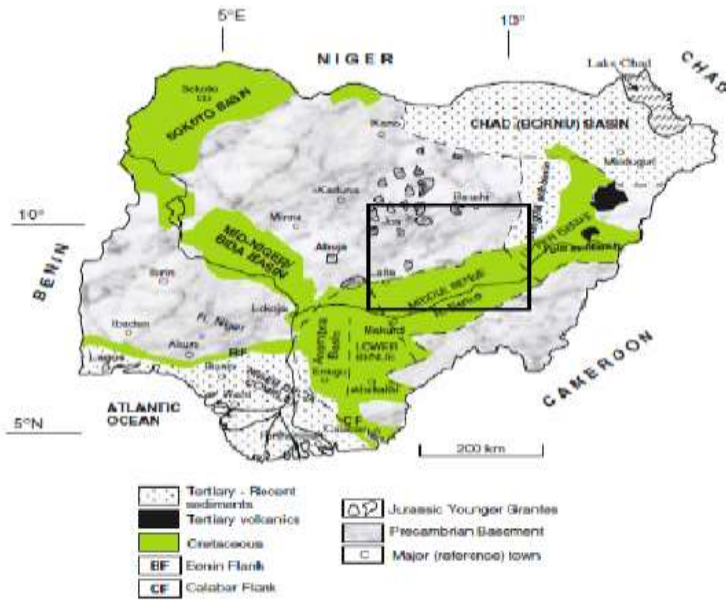
 Study Area  
 Surface Geothermal manifestation - Hot springs.

Fig.2: Geological setting and location of areas with major geothermal manifestation (Hot springs) in Nigeria (After Kurowska and Schoeneich, 2010).



 Study Area

Fig.3: Geological Map of Nigeria (Modified after Obaje, 2009) showing the study area.

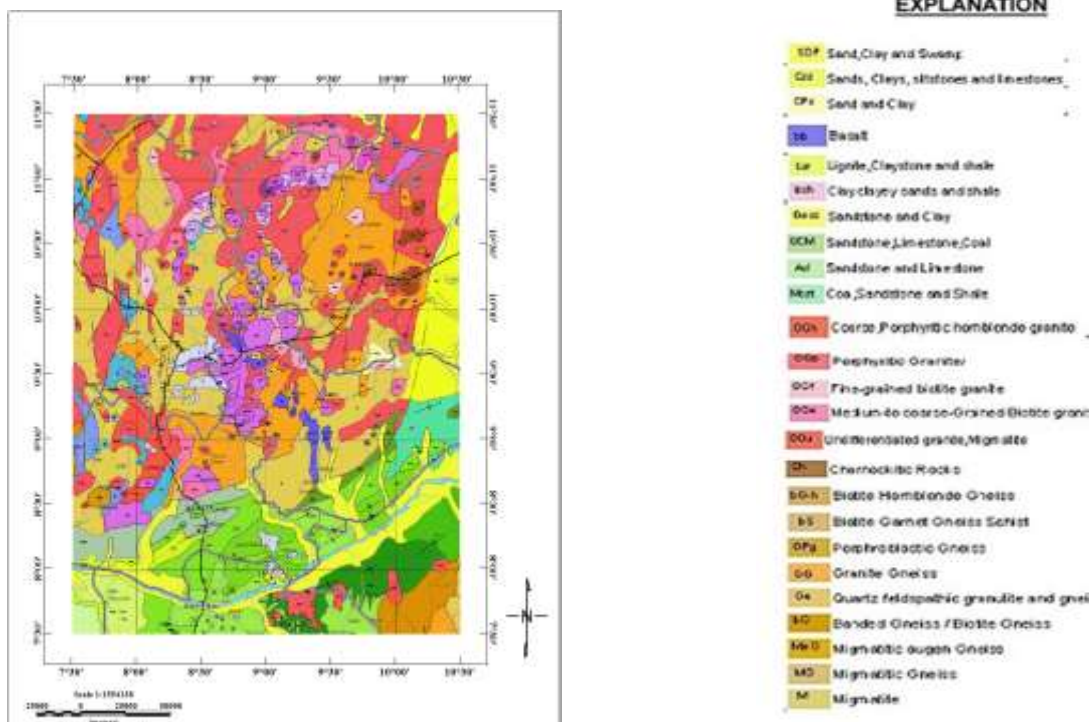


Fig.4: Geological Map of the study area (adapted after NGS, 2010)

**MATERIALS AND METHODS**

The high resolution aeromagnetic dataset, which consist of sheet 102 - 107, 124 - 129, 145 - 150, 166 - 171, 187 -192, 208 - 213, 229 – 234 and 249 – 254 utilized for this study was obtained as controlled maps of total magnetic intensity on a scale of 1:100000 compiled by the Nigerian Geological Survey Agency as a part of the nation-wide aeromagnetic survey between 2005 and 2010. The survey was flown in drape mode using real time global positioning system at a sensor mean terrain clearance of 80-100m. Traverse and Tie line spacing were 500m and 2000m respectively in NW-SE and NE-SW directions and the data were recorded at a sampling interval of 100m (NGSA, 2010) and stored in grid form. The study area is covered by forty-eight aeromagnetic maps of total-field intensity in ½° by ½° sheets. The data were initially pre-processed by Fugro Airborne Survey

and Consultant teams, pre-processing operation included micro levelling, removal of cultural effects as well as filtering for noise contents. The pre-processed data were quality controlled for isolated spikes and other spurious data which bear no correlation with geology. Butterworth filtering processing was applied to remove any possible cultural noise and other outrageous noise in order to increase the signal to noise ratio while minimizing other noise energies in the data. Total magnetic field intensity maps of the area comprising of the sheets (Fig.5) were plotted using Oasis Montaj software (version 8.4). The composite colour map (Fig.5) effectively displayed both long wavelength and short wavelength features. Fig.5 and Fig.6 are the total magnetic intensity map of the study area and the residual magnetic map of the study area respectively.

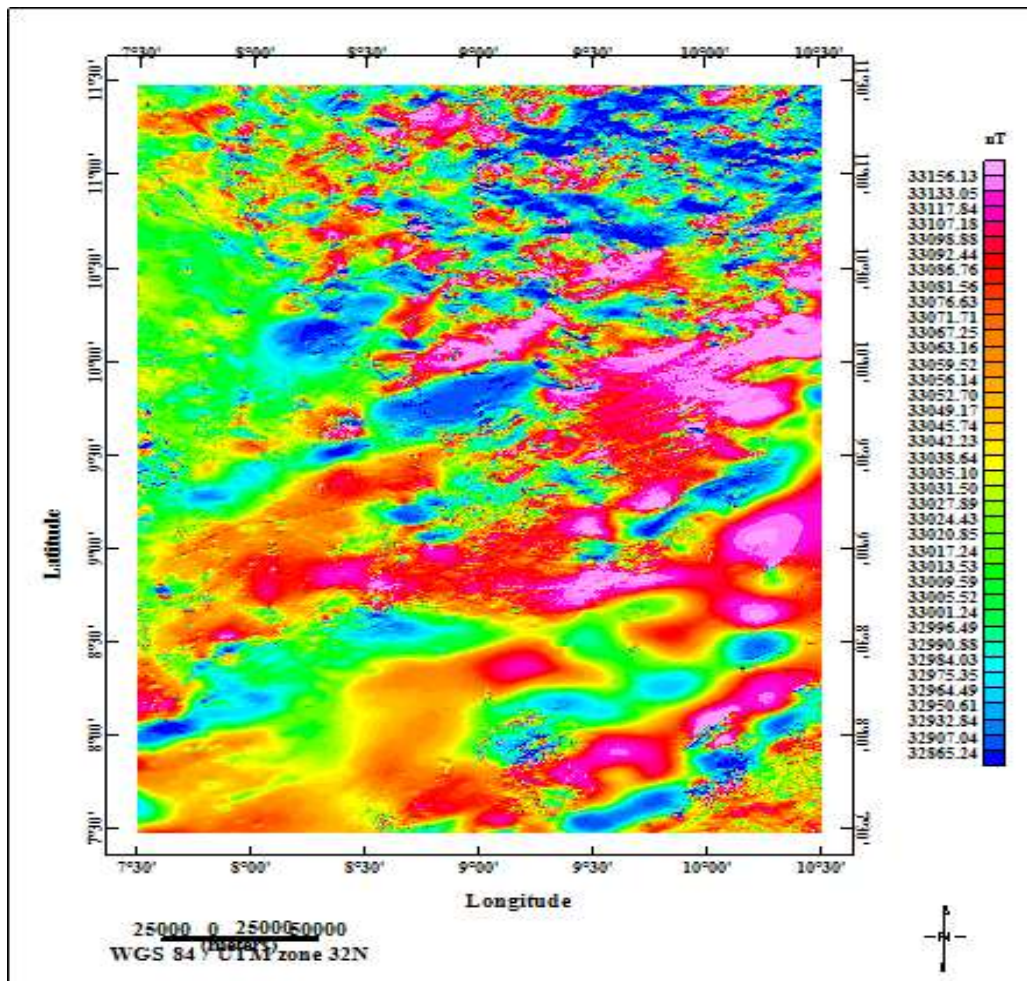


Fig.5: Total magnetic field intensity map of the study area.

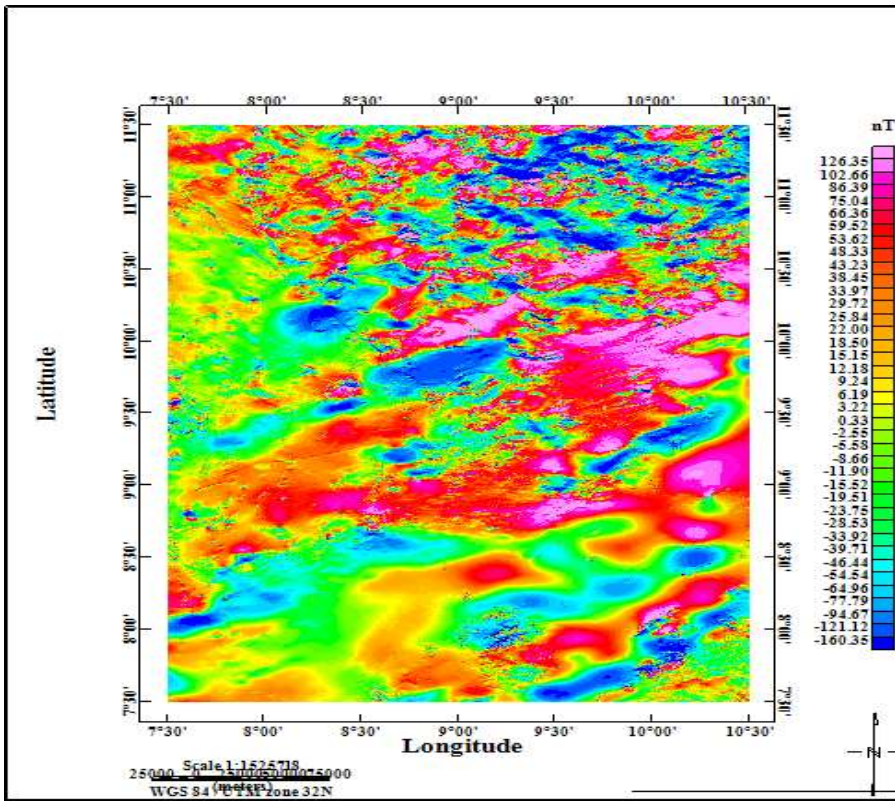


Fig.6: Residual magnetic field intensity map of the study area.

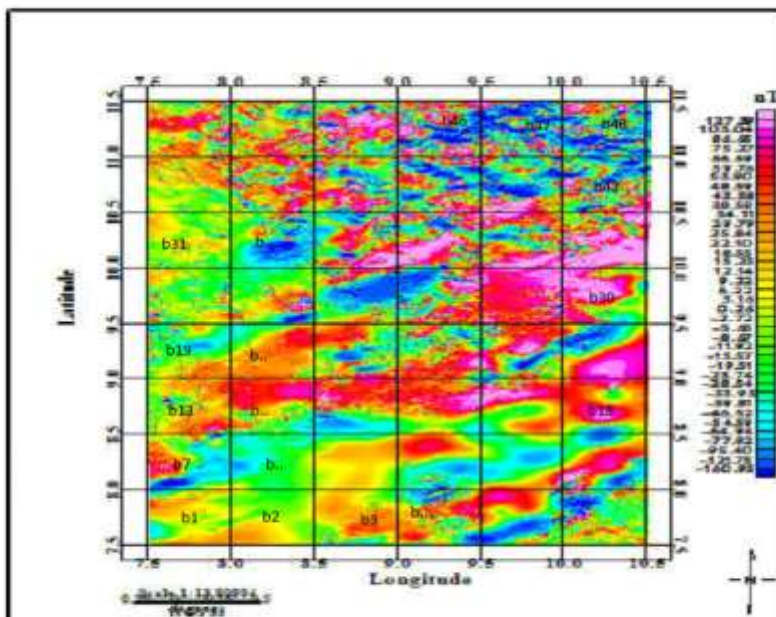


Fig.7: Residual magnetic field intensity divided into forty-eight square windows (55km by 55km each) from b1 to b48.

**Curie point depth estimation**

The methods for estimating the depth extent of magnetic sources are classified into two; those that examine the shape of isolated anomalies (Bhattacharyya and Leu, 1975) and those that examine the patterns of the anomalies (Spector and Grant, 1970). However, both methods provide the relationship between the spectrum of the magnetic anomalies and the depth to magnetic sources by transforming the spatial data into frequency domain. In this research, the method adopted is the later. To obtain the depth to Curie point, Spectral analysis of 2-dimensional Fourier transform of the aeromagnetic data has to be performed using Oasis Montaj software (version 8.4). To carry out Spectral analysis, the residual magnetic field intensity map of the study area was divided into forty-eight blocks (b1 – b48) (Fig.8), each block covers a square area of 55 by 55km, which represent a square grid of 32 by 32 data points and were padded and cosine tapered before Spectral evaluation for Curie and Heat flow assessments. Graphs of the logarithms of the spectral energies against frequencies were plotted using Grapher 8 software and Surfer 15 software was used to plot Curie point depth, Geothermal gradient and Heat flow graphs.

To perform the analysis, the first step, is to estimate the depth to Centroid ( $Z_o$ ) of the magnetic source from the slope of the longest wavelength part of the spectrum

$$\ln\left\{\frac{[\Delta T(|k|)^{1/2}]/|k|}{|k|}\right\} = \ln D - |k|Z_o \tag{1}$$

Where  $\ln\left\{\frac{[\Delta T(|k|)^{1/2}]/|k|}{|k|}\right\}$  is the radially averaged power spectrum of the anomaly,  $|k|$  is the wave number, and D is a constant.

The second step is the estimation of the depth to the top boundary ( $Z_t$ ) of that distribution from the slope of the second longest wavelength spectral segment (Okubo et al, 1985),

$$\ln\left[\frac{[\Delta T(|k|)^{1/2}]}{|k|}\right] = \ln B - |k|Z_t \tag{2}$$

Where  $\ln\left[\frac{[\Delta T(|k|)^{1/2}]}{|k|}\right]$  is the radially averaged power spectrum of the anomaly,  $|k|$  is the wave number, and B is the sum of constants independent of  $|k|$ . According to (Okubo *et al.*, 1985; Tanaka *et al.*, 1999), the basal depth ( $Z_b$ ) of the magnetic source was calculated from the equation below,

$$Z_b = 2Z_o - Z_t \tag{3}$$

The obtained basal depth ( $Z_b$ ) of magnetic sources in the study area is assumed to be the Curie point depth (Bhattacharyya and Leu, (1975) and Okubo et al, (1985) and the Graphs of the logarithms of the spectral energies for various blocks using the software were obtained from which table 1 was extracted as shown on Fig.9 below.

**Estimation of Heat flow and thermal gradient**

The heat flow and thermal gradient value was calculated in the study area; the calculation was expressed by Fourier's law (Fourier 1955) with the following formula.

$$q = \lambda \frac{dT}{dz} \tag{4}$$

Where q is the heat flow and  $\lambda$  is the coefficient of thermal conductivity. In this equation, it is assumed that the direction of the temperature variation is vertical and the temperature gradient  $\frac{dT}{dz}$  is constant. According to Tanaka, et al, (1999), the Curie temperature ( $\theta$ ) was obtained from the Curie point depth ( $Z_b$ ) and the thermal gradient  $\frac{dT}{dz}$  using the following equation;

$$\theta = \left\{\frac{dT}{dz}\right\}Z_b \tag{5}$$

Provided that there are no heat sources or heat sinks between the earth surface and the Curie point depth, the surface temperature is 0°C and  $\frac{dT}{dz}$  is constant. The Curie temperature depends on magnetic mineralogy. Although the Curie temperature of magnetite( $Fe_2O_4$ ), in view of that, the curie temperature is approximately 580°C, and an increase in titanium (Ti) content of titanomagnetite ( $Fe_{2-x}Ti_xO_3$ ) causes a reduction in Curie temperature (Nwankwo et al., 2011). In addition to that, from Equation (4) and Equation (5) a relationship was determined between the Curie point depth ( $Z_b$ ) and the heat flow (q) as follows.

$$q = \lambda \left\{\frac{\theta}{Z_b}\right\} \tag{6}$$

In this equation, the Curie point depth is inversely proportional to the heat flow (Tanaka et al. 1999; Stampolidis, et al., 2005). In this research, the Curie point temperature of 580 °C and thermal conductivity of  $2.5Wm^{-1} °C^{-1}$  as average for igneous rocks was used as standard (Nwankwo et al., 2011) in the study area. In order to compute the thermal gradient and heat flow of the region, Equation (6) was utilised. See Table 1 below.

Fig. 9 and Fig. 10, shows the graphs of the logarithms of the spectral energies for plots of blocks b39, b40, b45 and b46. The determined values of the basal depth or depth to the magnetic source  $Z_b$ , for these blocks using their determined  $Z_o$  and  $Z_t$  values in equation (3) are 11.3km, 8.51km, 7.63km and 11.2km. The Graphs of the logarithms of the spectral energies for the thirty-five blocks (c1 - c35) showing the determined values of  $Z_o$  and  $Z_t$  using Grapher 8 software can be found in appendix A. The results of the determined values of  $Z_o$ ,  $Z_t$  and  $Z_b$  for the thirty-five blocks are shown in table 1.

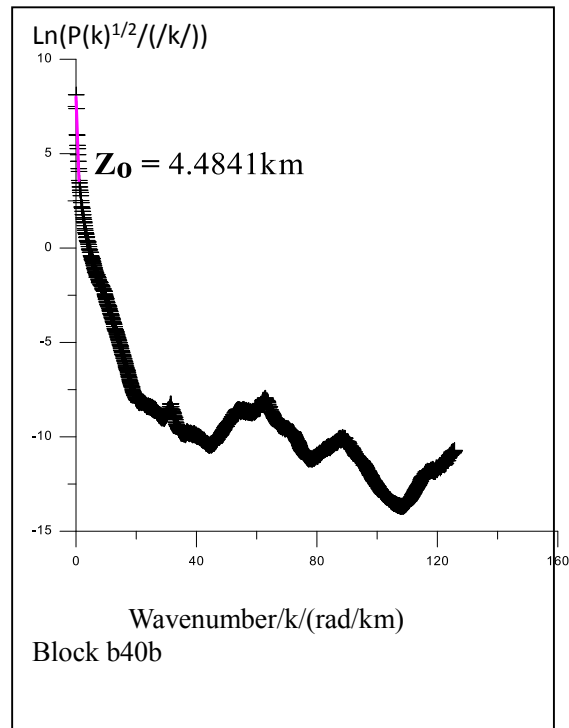
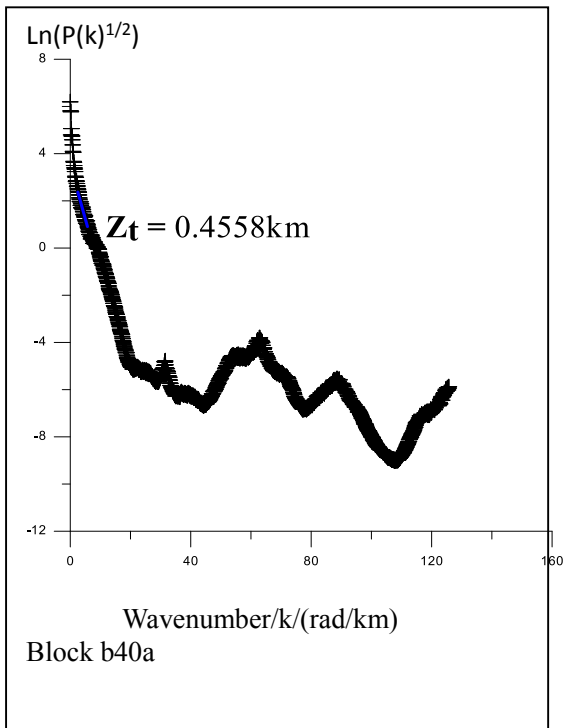
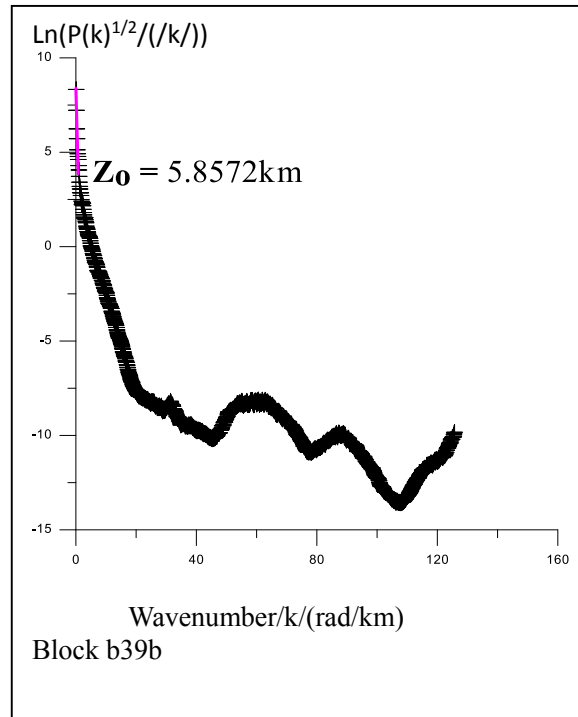
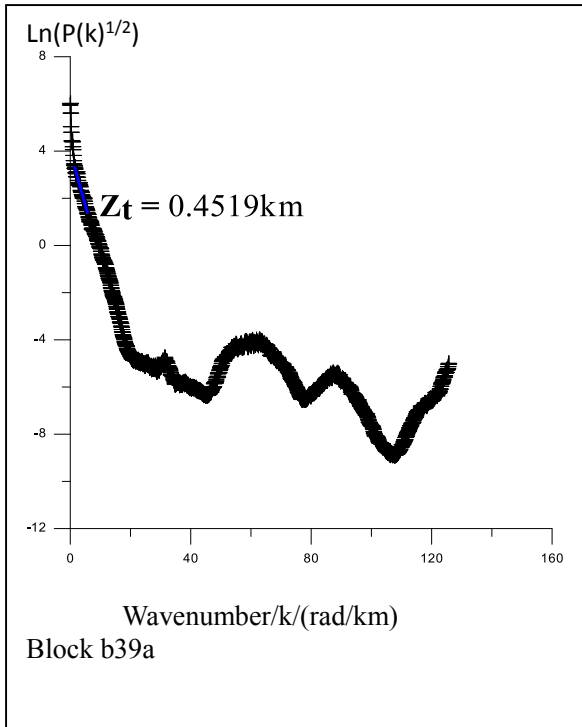


Fig. 9: Graphs of blocks b39, and b40, showing the determined values of  $Z_0$  and  $Z_t$  using Grapher 8 software.

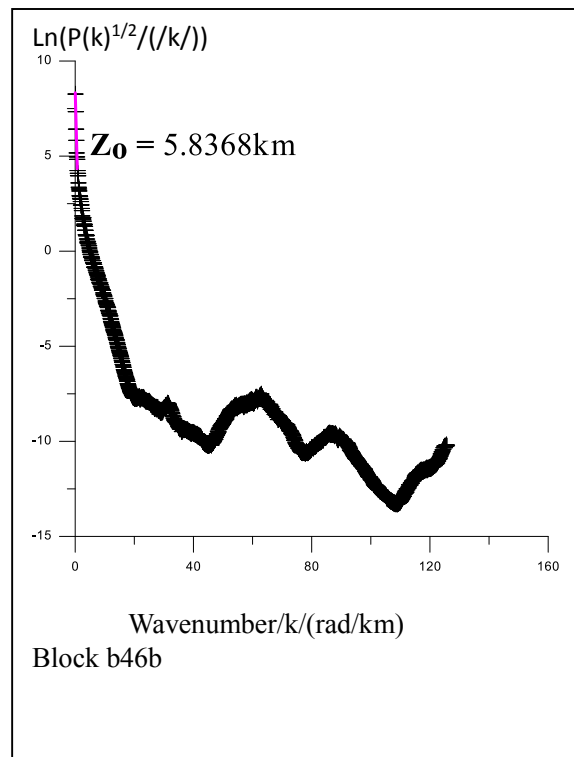
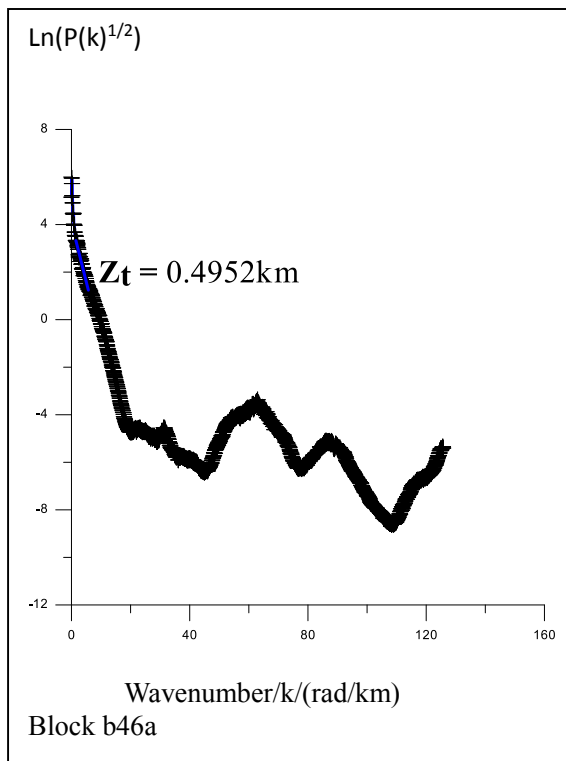
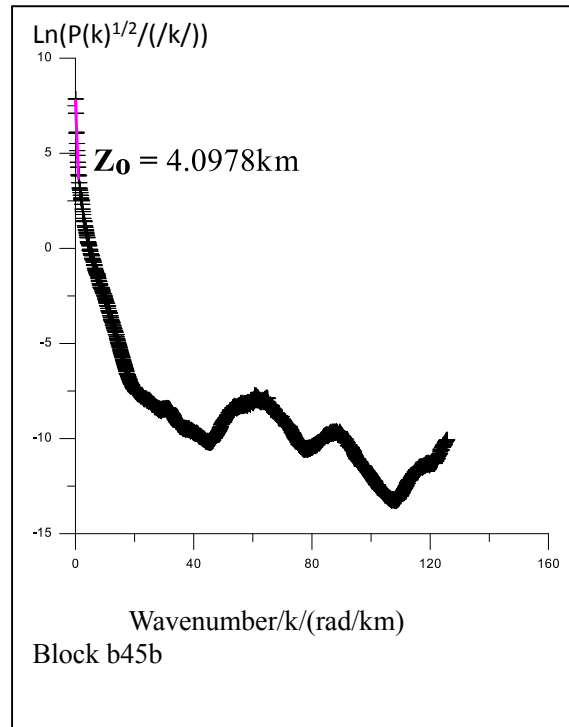
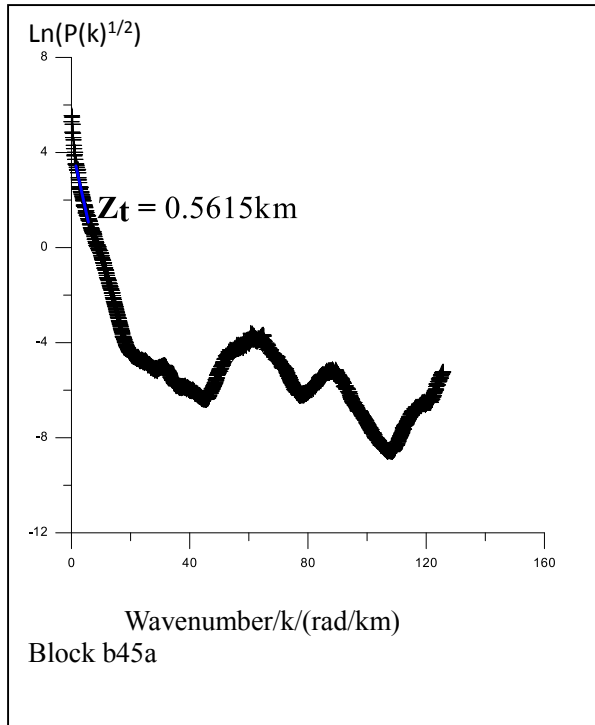


Fig. 10: Graphs of blocks b45, and b46, showing the determined values of  $Z_o$  and  $Z_t$  using Grapher 8 software



Table.1: Calculated Average Curie point depth, Geothermal gradient and Heat flow from spectral analysis

| BLOCK<br>(55km x<br>55km) | Depth to<br>Centroid<br>(Z <sub>0</sub> )<br>(Km) | Depth to top<br>boundary<br>(Z <sub>t</sub> )(km) | Curie<br>Depth<br>(Z <sub>b</sub> )<br>(Km) | Geothermal<br>gradient ( $\frac{dT}{dz}$ )<br>(°C/km) | Heat Flow (q)<br>(mWm <sup>-2</sup> ) |
|---------------------------|---------------------------------------------------|---------------------------------------------------|---------------------------------------------|-------------------------------------------------------|---------------------------------------|
| b1                        | 8.0314                                            | 0.7377                                            | 15.3251                                     | 37.846408832569                                       | 94.616022081422                       |
| b2                        | 7.9964                                            | 0.7570                                            | 15.2358                                     | 38.06823402775                                        | 95.170585069376                       |
| b3                        | 10.3952                                           | 0.3708                                            | 20.4196                                     | 28.40408235225                                        | 71.010205880624                       |
| b4                        | 10.0463                                           | 0.3647                                            | 19.7279                                     | 29.399986820696                                       | 73.499967051739                       |
| b5                        | 9.9044                                            | 0.3222                                            | 19.4866                                     | 29.764042983383                                       | 74.410107458459                       |
| b6                        | 14.5267                                           | 0.4892                                            | 28.5642                                     | 20.305137199712                                       | 50.762842999279                       |
| b7                        | 13.7469                                           | 0.4316                                            | 27.0622                                     | 21.432108254318                                       | 53.580270635795                       |
| b8                        | 14.3662                                           | 0.3933                                            | 28.3391                                     | 20.466422716318                                       | 51.166056790794                       |
| b9                        | 15.9907                                           | 0.4398                                            | 31.5416                                     | 18.388414030994                                       | 45.971035077485                       |
| b10                       | 14.7196                                           | 0.3024                                            | 29.1368                                     | 19.9060981302                                         | 49.765245325499                       |
| b11                       | 17.4091                                           | 0.3024                                            | 34.5158                                     | 16.803898504453                                       | 42.009746261133                       |
| b12                       | 11.2234                                           | 0.2513                                            | 22.1955                                     | 26.131423036201                                       | 65.328557590503                       |
| b13                       | 5.2893                                            | 0.3285                                            | 10.2501                                     | 56.584813806695                                       | 141.46203451674                       |
| b14                       | 7.7869                                            | 0.6612                                            | 14.9126                                     | 38.893284873194                                       | 97.233212182986                       |
| b15                       | 6.9032                                            | 0.4462                                            | 13.3602                                     | 43.412523764614                                       | 108.53130941154                       |
| b16                       | 7.7329                                            | 0.4477                                            | 15.0181                                     | 38.62006512142                                        | 96.55016280355                        |
| b17                       | 6.8137                                            | 0.5660                                            | 13.0614                                     | 44.405653299034                                       | 111.01413324758                       |
| b18                       | 6.7313                                            | 0.3048                                            | 13.1578                                     | 44.080317378285                                       | 110.20079344571                       |
| b19                       | 6.9175                                            | 0.4213                                            | 13.4137                                     | 43.239374669182                                       | 108.09843667295                       |
| b20                       | 9.9279                                            | 0.4890                                            | 19.3668                                     | 29.948158704587                                       | 74.870396761468                       |
| b21                       | 5.9267                                            | 0.3823                                            | 11.4711                                     | 50.561846727864                                       | 126.40461681966                       |
| b22                       | 6.8365                                            | 0.3873                                            | 13.2857                                     | 43.655960920388                                       | 109.13990230097                       |
| b23                       | 7.2783                                            | 0.5645                                            | 13.9921                                     | 41.451962178658                                       | 103.62990544664                       |
| b24                       | 7.4277                                            | 0.5953                                            | 14.2601                                     | 40.672926557317                                       | 101.68231639329                       |
| b25                       | 5.2989                                            | 0.4833                                            | 10.1145                                     | 57.343417865441                                       | 143.3585446636                        |
| b26                       | 5.9588                                            | 0.3386                                            | 11.579                                      | 50.090681405994                                       | 125.22670351498                       |
| b27                       | 8.3961                                            | 0.3562                                            | 16.436                                      | 35.288391336092                                       | 88.220978340229                       |
| b28                       | 5.0396                                            | 0.4995                                            | 9.5797                                      | 60.544693466392                                       | 151.36173366598                       |
| b29                       | 4.1622                                            | 0.3105                                            | 8.0139                                      | 72.374249741075                                       | 180.93562435269                       |
| b30                       | 6.5751                                            | 0.4687                                            | 12.6815                                     | 45.735914521153                                       | 114.33978630288                       |
| b31                       | 4.6539                                            | 0.4355                                            | 8.8723                                      | 65.372000495926                                       | 163.43000123981                       |
| b32                       | 7.2815                                            | 0.4802                                            | 14.0828                                     | 41.184991620984                                       | 102.96247905246                       |
| b33                       | 5.9621                                            | 0.4723                                            | 11.4519                                     | 50.646617591841                                       | 126.6165439796                        |
| b34                       | 6.2039                                            | 0.5679                                            | 11.8399                                     | 48.986900227198                                       | 122.46725056799                       |
| b35                       | 6.8776                                            | 0.4939                                            | 13.2613                                     | 43.736285281232                                       | 109.34071320308                       |
| b36                       | 5.8854                                            | 0.4095                                            | 11.3613                                     | 51.050495981974                                       | 127.62623995493                       |
| b37                       | 4.3036                                            | 0.4054                                            | 8.2018                                      | 70.716184252237                                       | 176.79046063059                       |
| b38                       | 5.1761                                            | 0.4244                                            | 9.9278                                      | 58.421805435242                                       | 146.05451358811                       |
| b39                       | 5.8572                                            | 0.4519                                            | 11.2625                                     | 51.49833518313                                        | 128.74583795782                       |
| b40                       | 4.4841                                            | 0.4558                                            | 8.5124                                      | 68.135895869555                                       | 170.33973967389                       |
| b41                       | 6.1948                                            | 0.4520                                            | 11.9376                                     | 48.585980431578                                       | 121.46495107894                       |
| b42                       | 4.9550                                            | 0.4959                                            | 9.4141                                      | 61.60971308994                                        | 154.02428272485                       |
| b43                       | 4.2503                                            | 0.3719                                            | 8.1287                                      | 71.352122725651                                       | 178.38030681413                       |
| b44                       | 4.4242                                            | 0.4801                                            | 8.3683                                      | 69.309178686233                                       | 173.27294671558                       |
| b45                       | 4.0978                                            | 0.5615                                            | 7.6341                                      | 75.97490208407                                        | 189.93725521018                       |
| b46                       | 5.8368                                            | 0.4952                                            | 11.1784                                     | 51.885779718028                                       | 129.71444929507                       |
| b47                       | 5.0831                                            | 0.4552                                            | 9.711                                       | 59.726083822469                                       | 149.31520955617                       |
| b48                       | 4.9580                                            | 0.5142                                            | 9.4018                                      | 61.690314620605                                       | 154.22578655151                       |

**RESULTS AND DISCUSSION**

Radially power spectrum was applied to the aeromagnetic data of the study area divided into 48 square blocks. The curie point depths, range from 7.63km to 34.52km, with a mean value of 14.79km, geothermal gradient, range from 16.80 °C km<sup>-1</sup> to 75.97°C km<sup>-1</sup>, with a mean value of 45.70 °C km<sup>-1</sup> and heat flow, range from 42.01 mWm<sup>-2</sup> to 189.94 mWm<sup>-2</sup>, with a mean value of 114.26 mWm<sup>-2</sup>. The curie point depth of the study area compare favourably with what was recorded over Sarti and environs of North-Eastern Nigeria (range from 24 to 28km, Kasidi and Nur (2012)), Jalingo and

Environs, North-Eastern part of Nigeria (range from 26 to 28km, Kasidi and Nur (2013)), the eastern Chad basin, Nigeria ((Mafa - Bama and Maiduguri - Gwoza areas) (range from 21 to 32 km , Anakwuba, et al., (2016))), the entire Bida Basin in north-central Nigeria (range from 16 to 30 km, Nwankwo and Sunday (2017)), part of the upper Benue trough corresponding to Kaltungo, Guyok, Lau and Dong areas, north eastern Nigeria (range from 12 to 34 km, Mohammed et al., (2019)) and the Upper Benue Trough (range from 24 to 33km, Nur et al., (1999)).

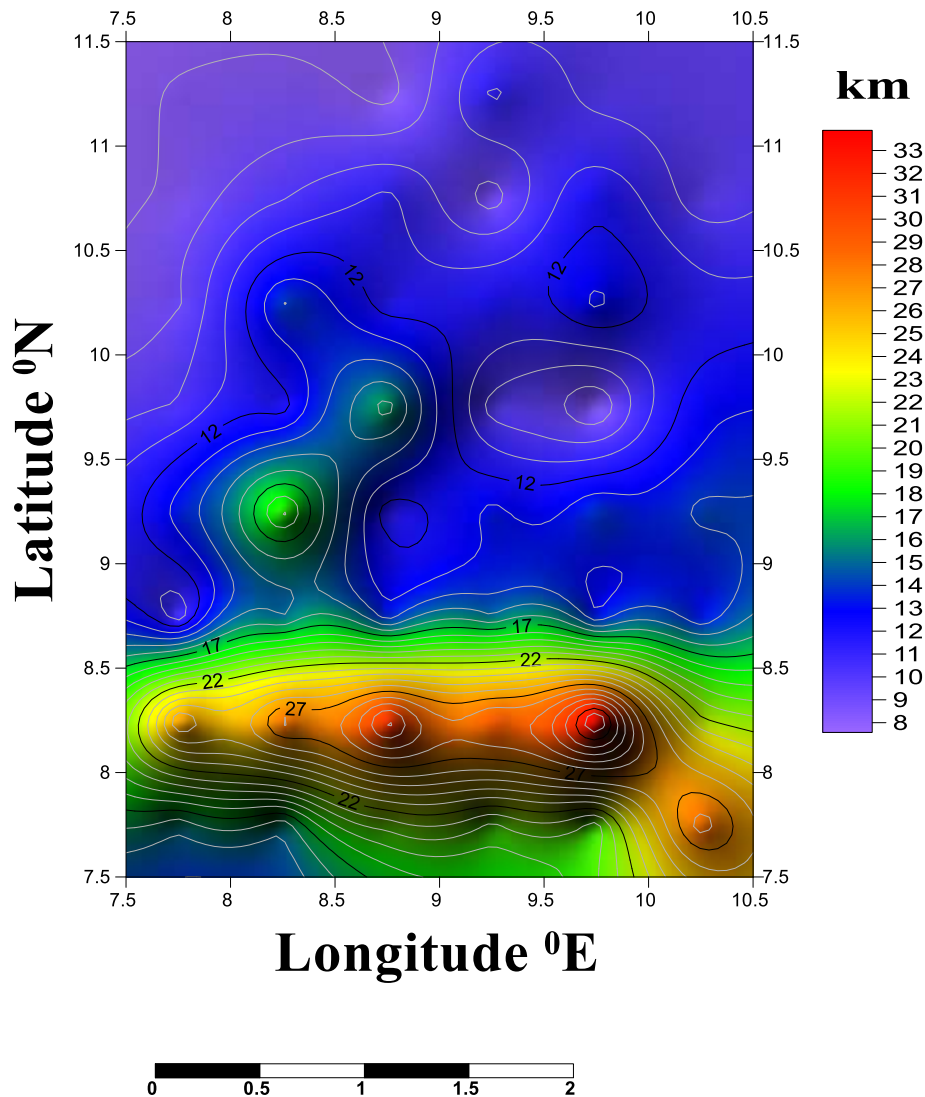


Fig.11: Curie point depth map of the study area using Surfer 8 software.

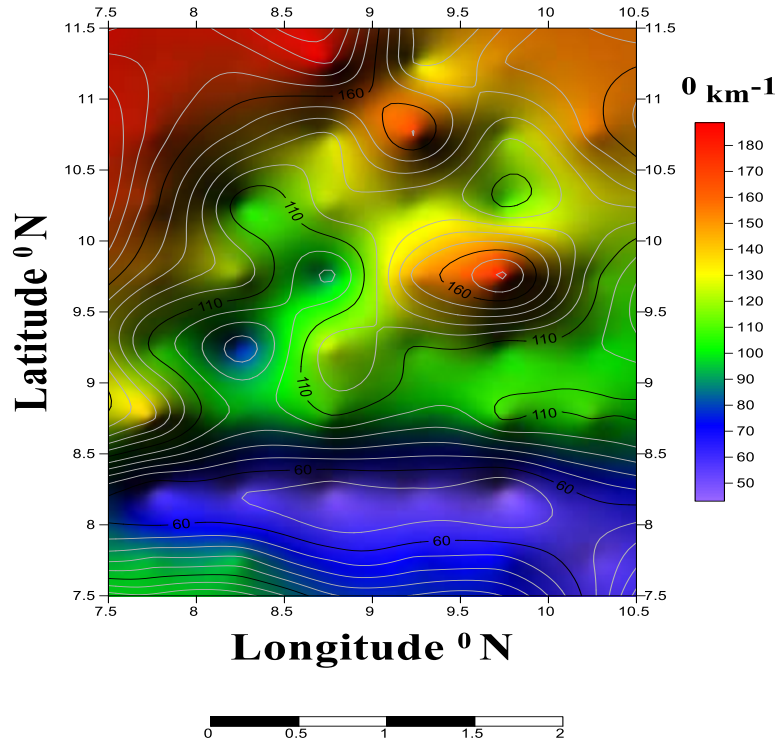


Fig.12: Geothermal gradient map of the study area using Surfer 8 software

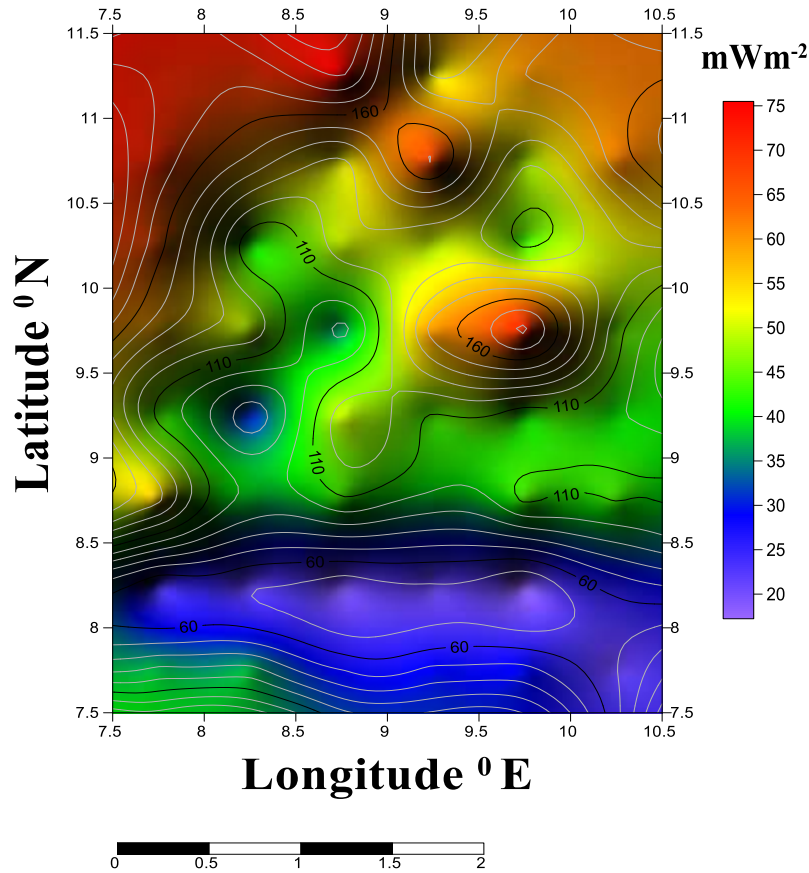


Fig.13: Heat flow map of the study area using Surfer 8 software.

## CONCLUSION

In this research, high resolution aeromagnetic data has been used to investigate the present of anomalies and the curie point depth of the study area. The quantitative (Spectral analysis) interpretation technique was chosen to achieve the outlined objectives of this research. The curie point depths has a mean value of 14.79km, a mean geothermal gradient of 45.70°C km<sup>-1</sup> and heat flow and a mean heat flow of 114.26 mWm<sup>-2</sup>. Fig. 8, show that, the curie point depth is shallower in the extreme northeast, southeast and part of the west of the study area. Also, Fig. 12, show the thermal gradient tends to be higher mainly in the north, central and extreme southeast of the study area and Fig. 13, show that, the heat flow tends to be higher mainly in the north, central and extreme southeast of the study area. The above characteristics of these areas according to Stein and Stein (1994) and Tanaka et al., (1999), reveals that, there might probably be good sources for geothermal and thereby recommended for both geothermal exploration and exploitation.

## REFERENCES

- Abdulsalam, N. N., Mallam, A. and Likkason, O. K. (2013). Evidence of some tectonic events in Koton Karifi area, Nigeria, from aeromagnetic studies. *Journal of petroleum and gas exploration research* (ISSN 2276-6510) vol. 3(1) pp. 7-15. <http://www.interestjournals.org/jpge> copyright 2013 international research journals.
- Abdullahi, M., Kumar, R. and Singh, K.U. (2019). Magnetic basement depth from high-resolution aeromagnetic data of parts of lower and middle Benue Trough (Nigeria) using scaling spectral method. *Journal of African Earth Sciences, Volume 150*. Pages 337-345. <https://doi.org/10.1016/j.jafrearsci.2018.11.006>.
- Adelana, A. M.S., Olasehinde, I.P., Bale, B.R., Vrbka, P., Edet, E.A. and Goni, B.I. (2008). An overview of the geology and hydrogeology of Nigeria. DOI: 10.1201/9780203889497.ch11. Retrieved 31<sup>st</sup> May, 2018.
- Alexander, R. (2017, November). Satellite Imagery: helping in identifying Geothermal potential in Ethiopia. Retrieved <http://www.thinkgeoenergy.com/satellite-imagery-helping-in-identifying-geothermal-potential-in-Ethiopia/>
- Anakwuba, E., Okeke, H., Chinwuko, I. and Onyekwelu, C. (2016). Estimation of Curie isotherm and heat flow of eastern Chad basin, Nigeria from spectral analysis of aeromagnetic data. SEG, International Conference and Exhibition, Barcelona, Spain, 3-6 April 2016.
- Bello, R., Ofoha, C. C. and Wehiuzo, N. (2017) . Geothermal Gradient, Curie Point Depth and Heat Flow Determination of Some Parts of Lower Benue Trough and Anambra Basin, Nigeria, Using High Resolution Aeromagnetic Data. *Physical Science International Journal* 15(2): 1-11.
- Bhattacharyya, B. and Leu, L.K. ( 1975). Analysis of magnetic anomalies over Yellowstone National Park. Mapping the Curie-point isotherm surface for geothermal reconnaissance. *J. Geophys. Res.* 80, 461–465.
- Black, R. (1980) Precambrian of West Africa. Episodes 4:3–8Burke KC, Dewey JF (1972). Orogeny in Africa. In: Dessauvage TFJ, Whiteman AJ (eds), Africa geology. University of Ibadan Press, Ibadan, pp 583–608
- Byerly, P.E.and Stolt, R.H. (1977). An attempt to define the Curie point isotherm in northern and central Arizona. *Geophysics* 42, 1394–1400.
- Carter, J. D., Barber, W. and Tait, E.A. (1963). The geology of parts of Adamawa, Bauchi and Bornu Provinces in north-eastern Nigeria. *Bulletin of the Geological Survey Nigeria*, 30.
- Chinwuko, A. I., Onwumesi, A. G., Anakwuba, E. K., Okeke, H. C., Onuba L.N., Okonkwo, C.C. Ikumbur, E. B. (2013). Spectral Analysis and Magnetic Modeling over Biu – Damboa, Northeastern Nigeria. *IOSR Journal of Applied Geology and Geophysics*, 1(1), 20- 28.
- Connard, G., Couch, R.and Gemperle, M.(1983). Analysis of aeromagnetic measurements from the Cascade Range in central Oregon. *Geophysics* 48, 376–390.
- Ekwueme, B. N. (1987). Structural Orientations and Precambrian deformation episodes of Uwet area, Oban massif. *Precambrian Research*, 34, 269–289.
- Eletta B.E. and Udensi E.E. (2012). Investigation of the Curie Point Isotherm from the Magnetic Fields of Eastern Sector of Central Nigeria. *Geosciences*, 2(4): 101-106 DOI:10.5923/j.geo.20120204.05 .
- Farnbauer, B. and Tietz, G.( 2000). The individuality of laterites developed on the Jos- Plateau/Central- Nigeria (in Deutsch). *Zbl. Geol. Palaeont. Tiel I, Heft 5/6*, 509–525.
- Fourier, J. (1955). *Analytical Theory of Heat*. Dover Publications, New York.
- Glassley, E. (2010). *Geothermal Energy: Renewable Energy and the Environment*, CRCPress, ISBN 9781420075700.
- Igwesi, I. D. and Umego, N. M. (2013). Interpretation Of Aeromagnetic Anomalies Over Some Parts Of Lower Benue Trough Using Spectral Analysis Technique. *International Journal of Scientific & Technology Research* volume 2, issue 8, Pp. 153-165.ISSN 2277-8616.

- Ikumbur, E. B., Onwuemesi, A. G., Anakwuba, E. K., Chinwuko, A. I., Usman, A.O. and Okonkwo, C. C. (2013). Spectral Analysis of Aeromagnetic Data over Part of the Southern Bida basin, West-Central Nigeria. *International Journal of Fundamental Physical Sciences*, 3(2), 27-31.
- Kasidi, S. and Nur, A. (2012). Curie depth isotherm deduced from spectral analysis of magnetic data over sarti and environs of North-Eastern Nigeria. *Sch. J. Biotechnol.* 1 (3), 49–56.
- Kasidi, S and Nur, A. (2013). Estimation of Curie Point Depth, Heat Flow and Geothermal Gradient Inferred from Aeromagnetic Data over Jalingo and Environs North – Eastern Nigeria. *International Journal of Science. Emerging Tech.* Vol-6. No. 6.
- Kebede, S.(1986). Results of temperature gradient survey and geophysical review of Corbetti geothermal prospect, EIGS.
- Kogbe, C. A. (1989). *Geology of Nigeria*. Rock View (Nigeria) Limited. Jos, Nigeria.
- Kurowska, E. and Schoeneich. K. (2010): Geothermal Exploration in Nigeria. Proceedings of World Geothermal Congress, 2010. Bali, Indonesia, 25-29 April 2010.
- Mohammed, A., Adewumi, T., Kazeem, A. S., Abdulwaheed, R., Adetona, A. A. and Usman, A. (2019). Assessment of geothermal potentials in some parts of upper Benue Trough northeast Nigeria using aeromagnetic data. *Journal of Geoscience, Engineering, Environment, and Technology*, [S.l.], vol. 4, no. 1, p. 7-15. ISSN 2541-5794. <<https://www.journal.uir.ac.id/index.php/JGEET/article/view/2090>>. Date accessed: 22 jan. 2020. doi: <https://doi.org/10.25299/jgeet.2019.4.1.2090>.
- Nur, A., Ofoegbu, C.O. and Onuoha, K.M. (1999). Estimation of depth to the Curie point isotherm in the Upper Benue Trough, Nigeria. *Jour. Mining and Geol.*35(1): 53 – 60.
- Nwankwo, L.I, Olasehinde, P.I and Akoshile, C.O.,(2011). Heat flow anomalies from the spectral analysis of Airborne Magnetic data of Nupe Basin, Nigeria. *Asian Journal of Earth Sciences*. Vol.1. No.1, pp. 1-6
- Nwankwo, L. and Sunday, J. A. (2017). Regional Estimation of Curie-point depths and succeeding geothermal parameters from recently acquired high-resolution aeromagnetic data of the entire Bida Basin, North-central Nigeria. *Geoth. Energ. Sci.*, 5, 1–9.
- Obaje, N. G. (2009). “Geology and Mineral Resources of Nigeria”. Nasarawa State University Dept. Geology and Mining Keffi Nigeria.p.50.
- Okubo, Y., Graf, R.J., Hansent, R.O., Ogawa, K. and Tsu, H.(1985). Curie point depths of the island of Kyushu and surrounding areas Japan. *Geophysics* 53, 481–494.
- Reyment, R. A. (1965). Aspects of the Geology of Nigeria. University of Ibadan Press, Nigeria, 145pp.
- Salako, A.K. (2012). Depth to Basement Determination Using Source Parameter Imaging (SPI) of Aeromagnetic Data: An Application to Upper Benue Trough and Borno Basin, Northeast, Nigeria. *Academic Research International* Vol. 5(3).
- Salem, A., Ushijima, K., Elsirafi, A. and Mizunaga, H. (2000). Spectral analysis of aeromagnetic data for geothermal Reconnaissance of Quseir area, northern red sea, Egypt. Proceedings World Geothermal Congress 2000. Kyushu - Tohoku, Japan.
- Shere, J.(2013). Renewable: The World-Changing Power of Alternative Energy. St Martin’s Press: New York, p. 201.
- Spector, A. and Grant, F.S. (1970). Statistical models for interpreting aeromagnetic data. *Geophysics* 35, 293–302.
- Stampolidis, A., Kane, I., Tsokas, G.N. and Tsourlos, P. (2005). Curie point depths of Ibania inferred from ground total field magnetic data. *Surv. Geophys.* 26, 461–480.
- Stein, C.A., Stein, S., 1994. Constraints on hydrothermal heat flux through the oceanic lithosphere from global heat flow. *J. Geophys. Res.* 99, 3081–3095.
- Tanaka, A., Okubo, Y., Matsubayashi, O. (1999). Curie point depth based on spectrum analysis of the magnetic anomaly data in East and Southeast Asia. *Tectonophysics* 306, 461–470.
- Tildy, B. (2015). /world-s- largest-geothermal-power-plant-opens-in-kenya. <http://www.powerengineeringint.com/articles/2015/02/world-s-largest-geothermal-power-plant-opens-in-kenya.html>. Retrieved 09/09/2017.



©2020 This is an Open Access article distributed under the terms of the Creative Commons Attribution 4.0 International license viewed via <https://creativecommons.org/licenses/by/4.0/> which permits unrestricted use, distribution, and reproduction in any medium, provided the original work is cited appropriately.